29th Congress of the International Council of the Aeronautical Sciences
St. Petersburg, Russia; September 7-12, 2014

ON SOUND ABSORPTION BY AN ACOUSTIC LINER WITH BIAS FLOW

C. Legendre* , L.M.B.C. Campos**
*Free Field Technologies S.A , **Instituto Superior Técnico (IST), Technical University of Lisbon

Keywords: *acoustic liners, shear flow, cross flow, sound propagation*

Abstract

A wave equation is obtained to describe the sound propagation in a unidirectional shear flow with linear velocity profile superimposed to a constant cross-flow, together with an impedance wall boundary condition, this represent the effect of a locally reacting liner with bias flow in presence of a shear flow. The wave equation is a third-order differential equation in the presence of cross-flow, and its general solution is a linear combination of three linearly independent MacLaurin series. The acoustic field in the boundary layer governed by the acoustic-vortical wave equation is matched through the pressure and horizontal and vertical velocity components to the acoustic field in a uniform free stream consisting of incident and reflected waves. In addition with the impedance boundary condition at the wall this specifies the pressure field in the whole domain and the reflection and transmission coefficients. These are plotted for several values of free stream and cross flow Mach numbers.

1 Introduction

Air inlets and exhaust nozzles of jet engines make extensive use of liners to absorb or attenuate sound. A locally-reacting acoustic liner can be represented by an impedance wall condition. In the present work, the combination of the three effects is presented, namely: (i) a plane flow over a flat impedance wall; (ii) a boundary layer with a unidirectional shear flow and linear velocity profile; and (iii) a uniform cross-flow representing the bias flow out of the perforated liner (figure 1). The pressure perturbation in the free stream consists of incident and reflected plane waves and it must be matched to the pressure field in the boundary layer in order to apply the impedance boundary condition at the wall, the latter specifies the reflection coefficient and thus the wave pressure perturbation in the whole flow, inside and outside the boundary layer. The acoustic-vortical wave equation specifying the pressure field in the boundary layer is at least of third order because, the sound is described by a second order wave equation allowing for propagation in opposite directions, the vorticity transport is specified by a first-order conservation equation along the streamlines in a potential homentropic flow (§2). In the case of sound in a unidirectional shear flow, the wave equation leads to a second-order differential equation for the dependence on the distance from the wall.

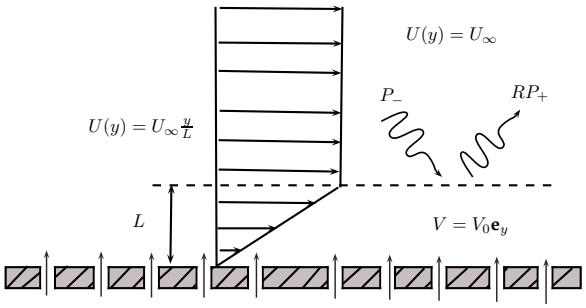

Fig. 1 : Sound propagation in a linear shear and cross layer profile.

This differential equation has a critical layer when the Doppler shifted frequency vanishes occurring when the horizontal phase velocity equals the velocity of the mean shear flow, so that the wave cannot further propagate. The presence of a cross-flow convects the wave away from this condition and therefore the acoustic-vortical wave equation has no singularity or critical layer(§2.1).

The pressure perturbation in the boundary layer is a linear combination of three solutions, each specified by Taylor series as a function of the distance from the wall. The three constants are specified by matching the pressure and horizontal and vertical velocity perturbations at the edge of the boundary layer to the sound field in the free stream(§3). This specifies the pressure perturbation in the boundary layer involving the reflection coefficient, which is determined from the impedance boundary condition at the wall (§4). The pressure perturbation as a function of the distance from the wall is plotted (figures 6,7) for several combinations of the of the free stream and cross-flow Mach numbers (§6.2). Finally, the effects of the free stream and cross-flow Mach numbers over the reflection and transmission coefficients are investigated (figures 8-11).

2 Acoustic wave equation with shear and cross flow

The starting point for the derivation of the acoustic-vortical wave equation is the fundamental equations of fluid dynamics, namely continuity, momentum and energy equations, in their classic forms in terms of velocity, pressure and density. Some hypothesis were taken in the derivation: (i) the viscous effects are neglected; and (ii) the fluid is considered adiabatic. Moreover, the mean flow is assumed to be plane and consist of a uniform bias or cross-flow orthogonal to a straight wall with velocity V_0 superimposed to a unidirectional shear flow parallel to the wall with a linear velocity profile in a boundary layer of thickness L matched to a uniform stream with velocity U_∞, as presented in figure 1. Thus, the mean flow $\mathbf{v}_0$ may be written as:

$$\mathbf{v}_0 = \mathbf{e}_y\, V_0 + \mathbf{e}_x\, U_0(y), \tag{1}$$

with the shear velocity U_0 expressed as follows:

$$U_0(y) = \begin{cases} U_\infty \frac{y}{L} & \text{if} \quad 0 \le y \le L, \\ U_\infty & \text{if} \quad L \le y < +\infty, \end{cases} \tag{2}$$

where y is defined as the distance perpendicular to the wall. Since the mean flow is steady and uniform in the wall direction a Fourier integral representation exists:

$$p(x,y,t) = P(y;k,\omega)e^{i(kx-\omega t)}, \tag{3}$$

where P is the pressure perturbation spectrum for a wave of frequency ω and horizontal wavenumber k at the distance y from the wall. Moreover, the linearised material derivative considering a linear shear flow superimposed to a constant bias flow (2) leads to the following relation:

$$\frac{d}{dt} = V_0 \frac{d}{dy} - i\omega_*(y), \qquad \omega_*(y) = \omega - kU_0(y), \tag{4a,b}$$

where ω_* is the wave Doppler frequency shifted by the horizontal shear flow alone. As a consequence, the acoustic-vortical wave equation in a linear shear flow with a uniform cross-flow may be written as*:

$$\begin{aligned} &\frac{d}{dt}\left(\frac{1}{{c_0}^2}\frac{d^2p}{dt^2} - \nabla^2 p\right) \\ &+\frac{dU_0}{dy}\left[2\frac{\partial^2 p}{\partial x \partial y} - \frac{V_0}{{c_0}^2}\frac{\partial}{\partial x}\left(\frac{dp}{dt}\right)\right] = 0. \end{aligned} \tag{5}$$

Substituting equation (3) in the wave equation (5) is obtained a third-order differential equation specifying the dependency of the acoustic spectrum P on the distance from the wall y with a cubic dispersion relation in k and ω:

$$\begin{aligned} &V_0\left({V_0}^2 - {c_0}^2\right)P''' + i\omega_*\left({c_0}^2 - 3{V_0}^2\right)P'' \\ &+\left[2ikU_0'\left({c_0}^2 + {V_0}^2\right) - 3V_0{\omega_*}^2 + V_0{c_0}^2k^2\right]P' \\ &+i\omega_*\left({\omega_*}^2 - k^2{c_0}^2 - 2ikV_0U_0'\right)P = 0. \end{aligned} \tag{6}$$

*See Campos, Legendre & Sambuc [4] equation (2.25).

2.1 The absence of the critical layer

The acoustic wave equation for unidirectional shear flow has been known for a long time [6, 8, 12]. Moreover, Lilley [10] proposed a third order wave operator that can be reduced to such wave equation when a unidirectional shear flow is considered. In this case, in absence of bias-flow, the wave equation (6) proposed in this work, reduces to the the acoustic wave equation in a unidirectional shear flow:

$$\omega_* P'' + 2kU_0{}' P' + \omega_* \left[(\omega_*/c_0)^2 - k^2 \right] P = 0. \tag{7}$$

It must be noticed that equation (7) is of the second order in $y-$direction. Moreover, equation (7) has a singularity when the coefficient of P'', i.e. the Doppler shifted frequency ω_*, vanishes. To interpret this physically, consider a wave of frequency ω and horizontal wave number k, hence horizontal phase speed $w = \omega/k$ propagating against a unidirectional shear flow. At the critical layer y_c when the horizontal phase speed equals the mean flow velocity $w = U(y_c)$ the Doppler shifted frequency vanishes $\omega_*(y_c) = 0$. Therefore, the wave can no further propagate, and the wave equation (7) has a singularity, implying one of the following possibilities: (i) the wave becomes evanescent beyond the critical layer that acts as a total reflector; or (ii) the wave is partly absorbed, partly reflected and partly transmitted as another mode able to propagate beyond the critical layer. In all cases the critical layer occurs at the point where the wave is "stopped" by the mean flow. The sonic condition in a potential flow is also a singularity of the acoustic wave equation.

On the other hand, applying a cross flow to the wave problem as described in figure 2, the wave is convected away from the critical layer and therefore the singularity is removed. Thus, the acoustic-vortical wave equation with cross-flow (6) has no singularity, i.e. the coefficient of the third-order derivative does not vanish, except if the cross flow reaches the sonic condition. The acoustic-vortical wave equation in a unidirectional shear flow is simpler in the presence of cross-flow, in the sense that it has no singularity, so it has solution as Taylor series valid in the whole flow region or the radius of convergence of the Taylor series is limited only by another singularity y_* due to another feature of the mean flow. In the absence of cross-flow the singularity at the critical layer would: either require a Frobenious-Fuch series around the critical layer with radius of convergence limited only by another singularity or restrict the Taylor series solution around another point to a radius of convergence limited by the critical layer. The presence of the cross-flow increases the order of the differential equation involved in the problem to three, and can lead to stiff solutions, even for small cross flow velocity that appears as a factor of the highest order derivative.

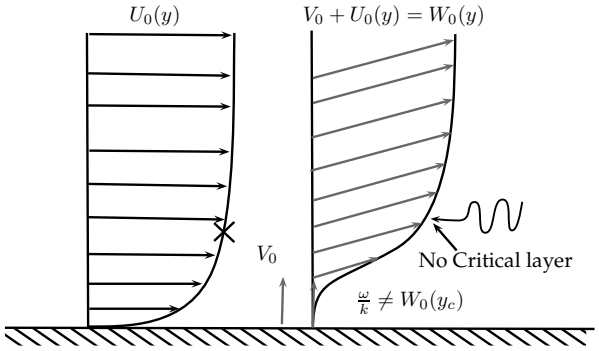

Fig. 2 : Graphical explanation of the existence of the critical layer. Acoustic propagation in shear and cross flow.

3 Acoustic pressure at the boundary layer and free stream

The acoustic-vortical wave equation in presence of bias and shear flow (6) applies inside the boundary layer, therefore the vertical position y describing the distance from the wall is normalized to the boundary layer thickness L, leading to the following pressure perturbation spectrum:

$$z = y/L, \qquad P(y;k,\omega) = Q(z), \tag{8a,b}$$

In addition, four dimensionless parameters are defined, namely: (i) the cross-flow Mach num-

ber (9a); (ii) the Mach number (9b); (iii) the dimensionless frequency or Helmholtz number (9c); and (iv) the dimensionless horizontal wavenumber or compactness (9d):

$$M_0 \equiv \frac{V_0}{c_0}, \qquad M_\infty \equiv \frac{U_\infty}{c_0}, \qquad \Omega \equiv \frac{\omega L}{c_0} = \frac{2\pi L}{\lambda}, \qquad \varepsilon \equiv kL = \Omega \cos\theta, \tag{9a-d}$$

where λ is the acoustic wavelength in an homogeneous medium at rest and θ is the angle of incidence of the plane wave at the free stream $z=1$, measured from the horizontal in the direction of the flow. Thus, considering the Helmholtz number, three regimes may be described: (i) for $\Omega \gg 1$ corresponding to sound rays in the boundary layer; (ii) for $\Omega \ll 1$ the boundary layer is considered acoustically thin; and (ii) for $\Omega \sim 1$ the wavelength is of the same order of magnitude than to the thickness of the boundary layer and therefore this represents the most interesting case. Furthermore, the dimensionless Doppler shifted frequency is expressed as:

$$\bar{\omega}_* \equiv \frac{\omega_* L}{c_0} = \frac{L}{c_0}\left[\omega - kU_0(y)\right] = \frac{\omega L}{c_0} - \frac{kU_\infty y}{c_0} = \Omega - \varepsilon M_\infty z. \tag{10}$$

Substitution of the dimensionless parameters and relations (9a-d,10) in equation (6) leads to the following third-order differential equation:

$$M_0\left({M_0}^2-1\right)Q''' + i\bar{\omega}_*\left(1-3{M_0}^2\right)Q'' + \left[2i\varepsilon M_\infty\left(1+{M_0}^2\right) - 3M_0\bar{\omega}_*^2 + M_0\varepsilon^2\right]Q' + i\bar{\omega}_*\left(\bar{\omega}_*^2 - \varepsilon^2 - 2i\varepsilon M_0 M_\infty\right)Q = 0. \tag{11}$$

The coefficient of the highest order derivative is a non-zero constant except for a bias flow at sonic speed; excluding this case the differential equation (11) has no singularities, and the solution exists as a MacLaurin series (12b) with infinite radius of convergence (12a):

$$z < \infty : \qquad Q(z) = \sum_{n=0}^{\infty} a_n z^n. \tag{12a,b}$$

substitution of (12b) in equation (11) leads to the recurrence formula for the coefficients a_n[†]. The recurrence formula shows that the first three coefficients a_0,a_1,a_2 are arbitrary. Thus, by choosing $(a_0,a_1,a_2) = (1,0,0)$, $(0,1,0)$ and $(0,0,1)$ leads to three linearly independent solutions denoted respectively by $Q_1(z) \sim \mathcal{O}(1)$, $Q_2(z) \sim \mathcal{O}(z)$ and $Q_3(z) \sim \mathcal{O}(z^)$. Hence, the solution for the acoustic pressure inside the boundary layer (13a) is a linear combination in the following form:

$$0 \le z \le 1 : \qquad Q_-(z) = B_1 Q_1(z) + B_2 Q_2(z) + B_3 Q_3(z), \tag{13a,b}$$

where B_1, B_2 and B_3 are arbitrary constants of integration. The three arbitrary constants of integration are obtained by matching the acoustic-vortical waves in the boundary layer to acoustic waves in the free stream given by:

$$p_+(x,y,t) = exp\left[i\left(kx - \omega t\right)\right] P_+(y)\,, \tag{14}$$

with: (i) the same frequency ω and horizontal wavenumber k as for the pressure perturbation of acoustic-vortical waves in the boundary layer (13a); (ii) the dependence on the distance from the wall consisting of a downward propagating wave with unit amplitude and an upward propagating wave whose amplitude is the reflection coefficient R:

$$L \le y < \infty : \qquad P_+(y) = e^{-i\kappa y} + R\, e^{i\kappa y}; \tag{15a,b}$$

(iii) the vertical wavenumber in the form:

$$\kappa = \sqrt{\frac{\omega}{c_0}\left(1 - M_\infty \cos\theta - M_0 \sin\theta\right)^2 - k^2}, \tag{16}$$

where θ is the angle of incidence, that appears also in the horizontal wavenumber (9d); (iv) this confirms that the vertical compactness:

$$\varphi \equiv \kappa L = \Omega\sqrt{\left[1 - M_\infty\cos\theta - M_0\sin\theta\right]^2 - \cos^2\theta} \tag{17}$$

[†]see Campos, Legendre & Sambuc [4], equation (3.7).

involves the dimensionless frequency (9c) and the angle of incidence θ. Consequently, the acoustic wave field at the free stream (18a) may be rewritten as follows :

$$1 \leq z < \infty : \qquad Q_+(z) = e^{-i\varphi z} + R\, e^{i\varphi z}. \tag{18a,b}$$

The solution at the free stream (18b) is matched to the acoustical-vortical wave field (13b) in the boundary layer by the continuity of the pressure perturbation and its first two derivatives:

$$Q_-(1) = Q_+(1), \qquad Q'_-(1) = Q'_+(1), \qquad Q''_-(1) = Q''_+(1). \tag{19a-c}$$

These conditions (19a-c) are equivalent to the continuity of the pressure P and horizontal U and vertical V velocity perturbations at the edge of the boundary layer[‡].

4 Impedance boundary condition for locally reacting liner

The impedance boundary condition at the wall $y = 0$ in terms of the admittance may be expressed as follows:

$$V(0) = -\bar{A}P(0) : \quad P'(0) = -\rho_0 V_0 V'(0) + i\omega\rho_0 V(0), \tag{20a,b}$$

leading to an expression in terms of the pressure perturbation only:

$$\left(1 - \rho_0 V_0 \bar{A}\right) P'_-(0) = -i\omega\rho_0 \bar{A} P_-(0). \tag{21}$$

Also, the boundary condition (21) may be expressed in terms of dimensionless parameters as follows:

$$A \equiv \rho_0 c_0 \bar{A} : \quad (1 - M_0 A)\, Q'_-(0) = -i\Omega A Q_-(0), \tag{22a,b}$$

involving: (i) the specific admittance (22a) obtained dividing by that of a plane wave; (ii) the cross flow Mach number (9a) and dimensionless frequency (9c). Similarly, the transmission coefficient is defined:

$$T = \frac{Q_-(0)}{Q_+(L)}, \tag{23}$$

as the ratio of the pressure perturbations at the wall and in the free stream at the edge of the boundary layer. This completes the determination of the pressure perturbation in the whole flow outside and inside of the boundary layer, and of the scattering coefficients consistent with an impedance wall boundary condition.

5 Conditions in the free stream: Zone of silence and propagation sectors

Real values of the vertical wavenumber (16) correspond to the propagation zone(s) at the free stream, otherwise imaginary vales correspond to the zone(s) of silence where the sound waves are evanescent. These zones(s) of silence and propagation alternate and correspond to angular sectors depending on M_0 and M_∞. The boundaries between the zone(s) of silence and propagation zone(s) are the roots of the equation (17), that is a periodic transcendental equation, that would have to be solved by means of numerical methods. The roots of equation (17) are given by the solution of the following formula:

$$\left(1 \pm 2M_\infty + {M_0}^2 + {M_\infty}^2\right) \cos\theta_{\pm\pm} = M_\infty \pm 1 \pm M_0 \sqrt{{M_0}^2 + {M_\infty}^2 \pm 2M_\infty}, \tag{24a-d}$$

where the second $\pm$ applies to M_0 and the first $\pm$ to the remaining terms.

As a first example, consider $M_\infty = 2.0$ in the absence of cross-flow $M_0 = 0$ as depicted in figure 3a, there is only one real angle $\theta_+ = 70.52°$ separating a zone of silence in the downstream arc $0 \leq \theta \leq \theta_+$ from a propagation zone $\theta_+ < \theta \leq 180°$ in the upstream arc. Moreover, a second example with a free stream $M_\infty = 2.0$ and a cross-flow $M_0 = 0.3$ Mach numbers is depicted in figure 3b and leads to

[‡]See Campos Legendre & Sambuc [4], section §3-c.

the angles $\theta_{--} = 33.39°$ and $\theta_{+-} = 76.33°$; the vertical wavenumber is imaginary for $\theta = 60°$ in this range and real for $\theta = 30°$ and $90°$ outside this range. Thus (figure 3b) there are downstream $0° < \theta < 33.39° = \theta_{--}$ and upstream $\theta_{+-} = 76.33° < \theta < 180°$ propagation zones, with a zone of silence in between $\theta_{--} = 33.39° < \theta < 76.33° = \theta_{+-}$.

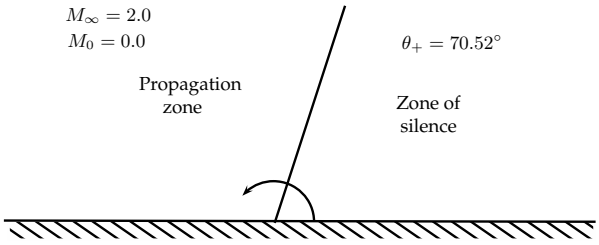

(a) Zone(s) for $M_\infty = 2.0$ and $M_0 = 0$

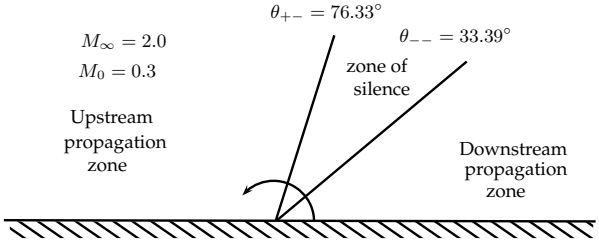

(b) Zone(s) for $M_\infty = 2.0$ and $M_0 = 0.3$

Fig. 3 : Examples of propagation zones and zones of silence with (b) and without (a) cross flow.

The distinction between propagation zones and zones of silence applies strictly in a uniform stream where the vertical wavenumber is constant, corresponding: (i) to real values to upward $\exp(i\kappa y)$ and downward $\exp(-i\kappa y)$ waves; (ii) to imaginary values $\kappa = i\,|\,\kappa\,|$, when the divergent solution $\exp(-i\kappa y) = \exp(|\,\kappa\,|\,y)$ is discarded and only the evanescent wave $\exp(i\kappa y) = \exp(-\,|\,\kappa\,|\,y)$ is retained. In a shear flow the distinction is less clear, since the waveforms are not sinusoidal in the $y-$direction and a vertical wavenumber strictly does not exist. A local varying vertical wavenumber $\kappa(y)$ would exist in the ray limit of the weak shear on a wavelength scale, that is $\Omega^2 \ll 1$ in (9c); this would break down for $\Omega \sim 1$ or $\Omega < 1$. Thus it may be appropriate to plot wave fields into the zones of silence since waves can penetrate these regions in the boundary

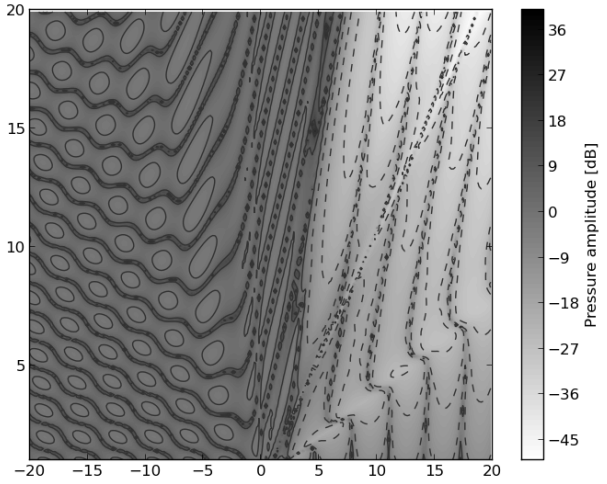

(a) Pressure map in the free stream.

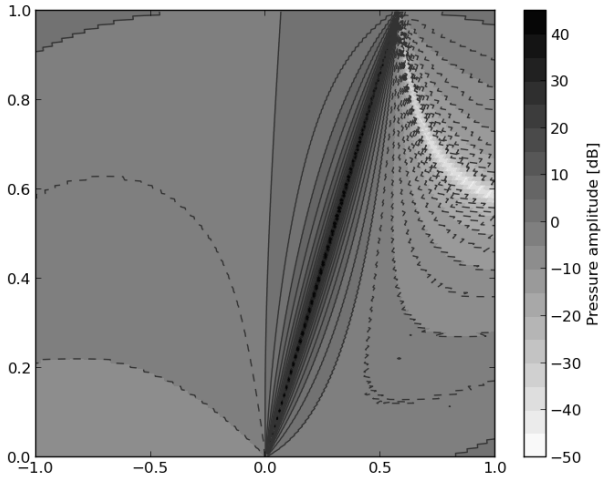

(b) Pressure map in the boundary layer

Fig. 4 : Pressure maps for $M_0 = 0.0$ and $M_\infty = 2.0$ corresponding to figure 3a.

layer. The pressure fields may be compared in: (i) the uniform free stream where a zone of silence exists; (ii) in the boundary layer where the non-uniform flow excludes the existence of a zone of silence in a strict sense. The two cases with (figure 3a) and without (figure 3b) bias flow are illustrated in the figures 4,5 with free stream zone in the top and the boundary layer zone in the bottom of each figure. The contour plots for the modulus for the amplitude of the acoustic pressure are shown: (i) using (25a) in the free stream, so that at the boundary between the zone of silence and the upstream and downstream propagation zones

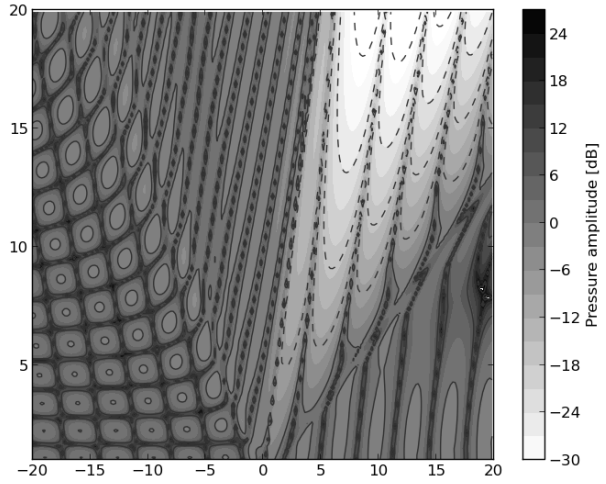

(a) Pressure map in the free stream.

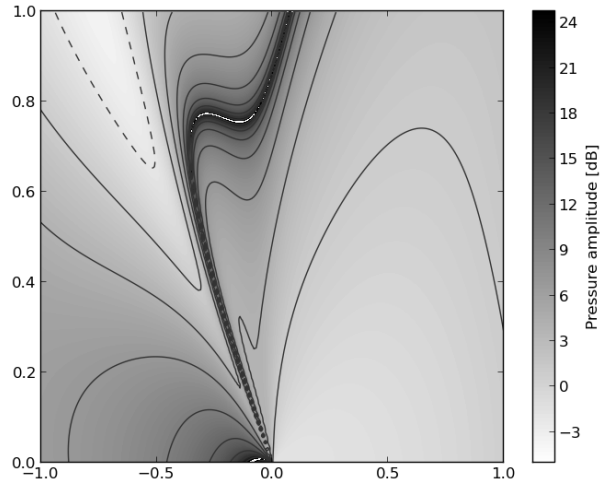

(b) Pressure map in the boundary layer

Fig. 5 : Pressure maps for $M_0 = 0.3$ and $M_\infty = 2.0$ corresponding to figure 3b.

$\varphi = 0$ and the value if S_+ is zero:

$$S_\pm(z) = 10\log\left[\frac{Q_\pm(z)}{1+R}\right]; \qquad (25a,b)$$

(ii) the boundary layer is used with the same normalization S_- (25b). In both plots the horizontal x and vertical y coordinates respectively along and perpendicular to the wall are made dimensionless by dividing by the thickness of the boundary layer. In the plots in figures 4,5 polar coordinates are taken and the pressure is represented by:

$$S_\pm(x,y) = e^{ikx}S_\pm(z) = e^{ikr\cos\theta}S_\pm\left(\frac{r}{L}\sin\theta\right). \qquad (26c)$$

The top plots in the figures 4,5 show the pressure amplitude in a large region of the free stream $-20 \le x/L \le 20$ by $1 \le y/L \le 20$ above the boundary layer. The boundary layer (bottom plots in figures 4,5) corresponds to an horizontal strip $0 \le y/L \le 1$. The pressure amplitude in the shear and cross flow in the boundary layer is depicted inside a smaller box $-1 \le x/L \le 1$ by $0 \le y/L \le 1$.

In the top of figures 4,5 the amplitude of the pressure shows a clear distinction between: (a) the zone of silence downstream and propagation zone upstream; (b) the zone of silence between upstream and downstream propagation zones. In all cases the pressure amplitude is much lower in the zone of silence with a sharp transition towards the propagation zone(s). On the bottom of figures 4,5, the pressure amplitude in the boundary layer with shear and cross flow: (figure 4) is fairly smooth in the absent of the bias flow; (figure 5) the bias flow causes some concentration of the pressure. In all cases the acoustic "zone of silence" has been destroyed by the vortical modes in the boundary layer.

6 Pressure field and scattering coefficients

6.1 Baseline case

The baseline parameters are taken as: (i) the sound speed (27a) in sea level atmospheric conditions; (ii)(iii) a high subsonic free stream (27b) with a much smaller bias velocity (27c); (iv) a boundary layer of moderate thickness (27d); (v) a wave frequency of $1\mathtt{kHz}$ in the part of audible range $20\mathtt{Hz} - 20\mathtt{kHz}$ more sensitive to noise (27e); (vi) a wall impedance (27f) or inverse of wall admittance combining resistance and inductance:

$$\{c_0, U_\infty, V_0\} = \{340, 272, 20.4\}\,\mathtt{m}*\mathtt{s}^{-1},$$
$$L = 0.05\,\mathtt{m},\ \frac{\omega}{2\pi} = 1.08\,\mathtt{kHz},\ \frac{1}{A} = 1+i. \qquad (27a\text{-}f)$$

These are typical values as order of magnitude of conditions in the inlet and exhaust ducts of

modern jet engines, where the acoustic liners with bias flow are used to attenuate the sound; for example precise values of the specific admittance depend on frequency and may not be available for a specific application, but it is known that the real and imaginary parts do not usually exceed unity. The preceding base-

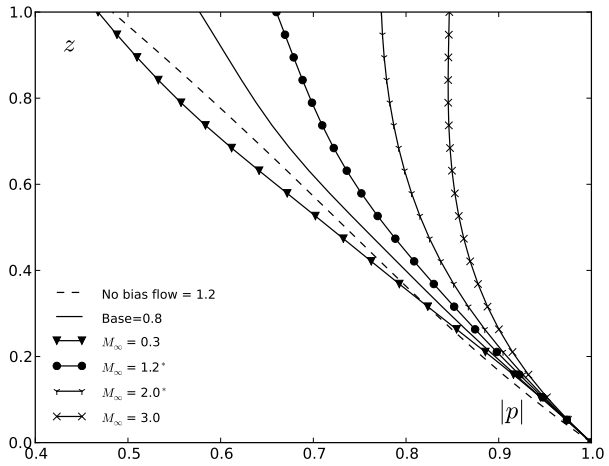

(a) Amplitude of normalized acoustic pressure.

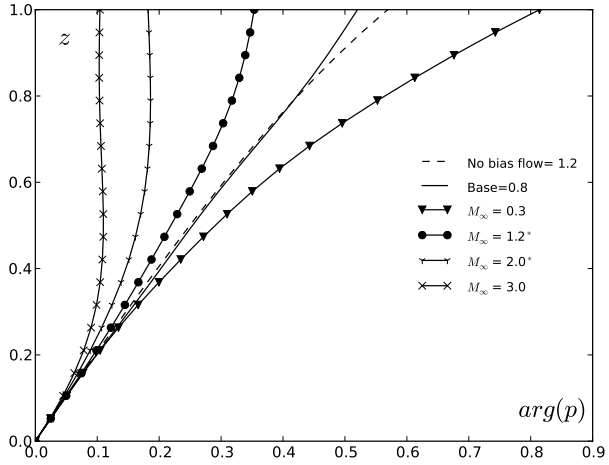

(b) Phase of normalized acoustic pressure.

Fig. 6 : Dimensionless distance from the wall as the vertical axis and acoustic pressure normalized to the wall value as horizontal axis, illustrating the profile of the modulus (top) that start at $z = 0$, $\mid p(0) \mid = 1$ and phase (bottom) that starts at $z = 0$, $arg\{p(0)\} = 0$. The baseline case is used, and four values for the core flow Mach number are considered (29a), all with bias flow (28b). The case without bias flow $M_0 = 0.0$ and free stream Mach number $M_\infty = 1.2$ appears as the dashed line.

line values (27a-f) serve only to calculate the reference values of the four dimensionless parameters, namely the specific impedance (27f) and: (i/ii) the free stream (28a) and cross flow (28b) Mach numbers; (iii) the dimensionless frequency(28c):

$$M_\infty \equiv \frac{U_\infty}{c_0} = 0.8, \quad M_0 \equiv \frac{V_0}{c_0} = 0.06, \quad \Omega \equiv \frac{\omega L}{c_0} = 1. \tag{28a-c}$$

The bias flow M_0 and the shear flow M_∞ will each be varied in turn over a sufficiently wide range to cover most aeronautical applications, so that the choice of starting numbers (28a-b) is not critical. Therefore, the cases with cross-flow are considered for all combinations of the free stream (29a) and cross-flow (29b) Mach numbers:

$$M_\infty = 0.3, 0.8, 1.2, 2.0, 3.0; \quad M_0 = 0.03, 0.06, 0.3, 0.8, 2.0. \tag{29a,b}$$

The dimensionless parameters (28a-c) specify the scattering coefficients, namely the amplitude and the phase of the reflection and transmission coefficients as a function of the angle of incidence in the full range of directions.

6.2 Results

The acoustic pressure normalized to the wall value is plotted as a function of dimensionless distance from the wall within the boundary layer in the figures 6,7 with the amplitude in the top and the phase in the bottom. In all figures appear, besides the baseline case (28a-c) with bias flow also the comparable case without bias flow in order to assess the importance of the cross flow. The cases without bias flow are different in each figure 6-7 leading to five distinct comparisons with bias flow. The baseline concerns $\theta = 60°$ propagation downstream and the cases with and without flow bias flow are compared for a free stream Mach number $M_\infty = 1.2$ in the figure 6. The top plot shows that the curvature is opposite in the case with (line with blobs) and without (dashed line) bias flow; thus the bias flow causes a slower decrease of the acoustic pressure away from

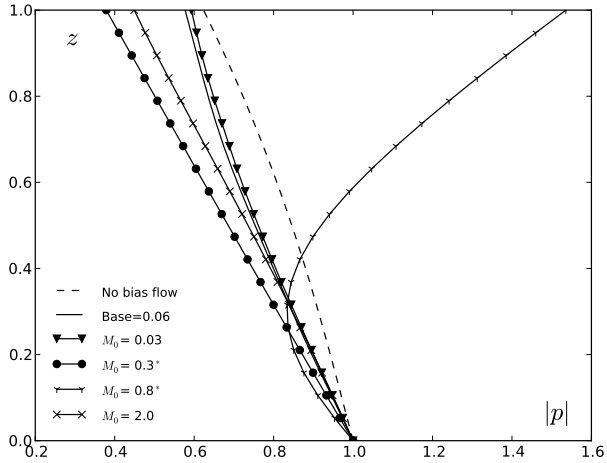

(a) Amplitude of normalized acoustic pressure.

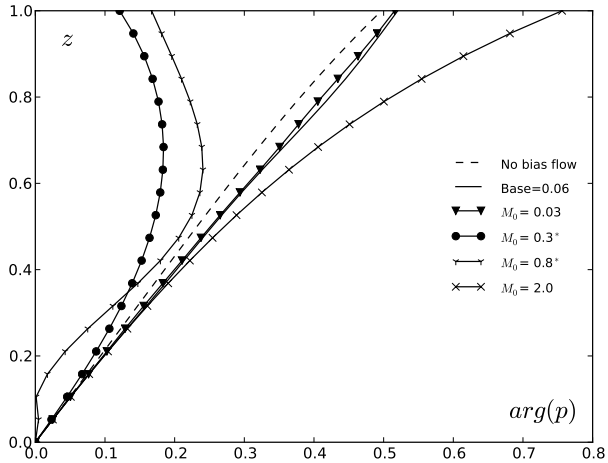

(b) Phase of normalized acoustic pressure.

Fig. 7 : As figure 6, but using four values for cross flow Mach number are considered (29b).

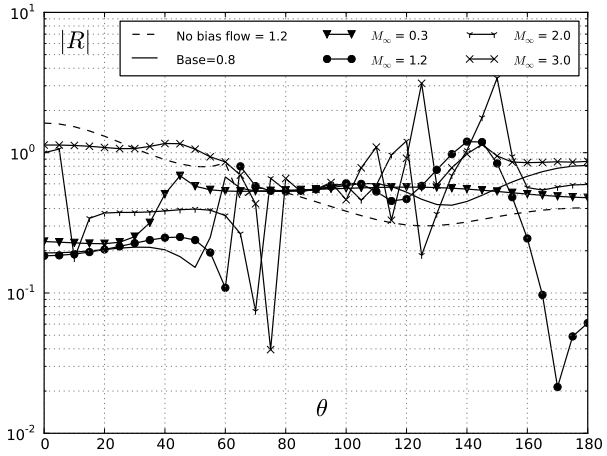

(a) Amplitude of reflection coefficient.

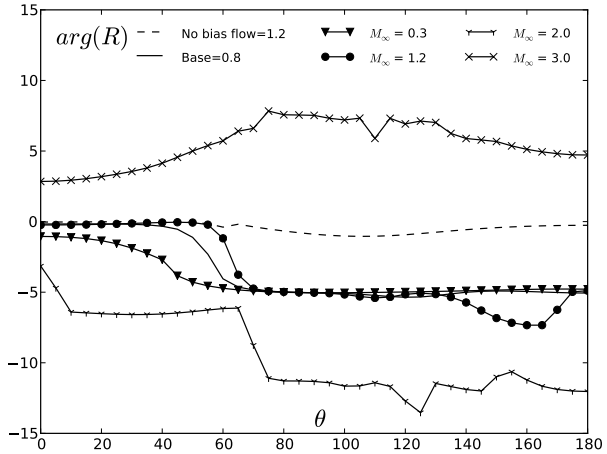

(b) Phase of reflection coefficient.

Fig. 8 : Reflection coefficient versus angle of incidence. The baseline case is used, and four values for shear Mach number are considered (29a), all with bias flow. The case without bias flow corresponds to $M_\infty = 1.2$ and is represented by the dashed line.

the wall. In the presence of bias flow the pressure decreases away from the wall more slowly for larger free stream Mach numbers (figure 6) while the phase varies more slowly; the cases marked with asterisk corresponding to the zone of silence in the free stream do lie among the others within the boundary layer as a continuous variation. The bottom of the figure 6 shows that the phase of the acoustic pressure varies almost linearly with the distance from the wall for lower Mach numbers; for larger Mach numbers the phase is non-linear indicating strong sound refraction effects. Concerning the comparison of the phase of the acoustic pressure like the amplitude, it is larger without than with bias flow. It should be borne in mind that the Mach number of the bias flow is small, and thus its main effect is to remove the critical layer at the condition of zero Doppler shifted frequency for the horizontal core flow. In spite of the smallness of the Mach number of the bias flow is has a detectable effect on the acoustic pressure, both for the amplitude (top of the figure 6) and for the phase (bottom of the figure 6).

To make more visible the effects of cross-flow the corresponding Mach number is given larger values well in excess of a typical bias flow, and more representative of a fluidic jet.

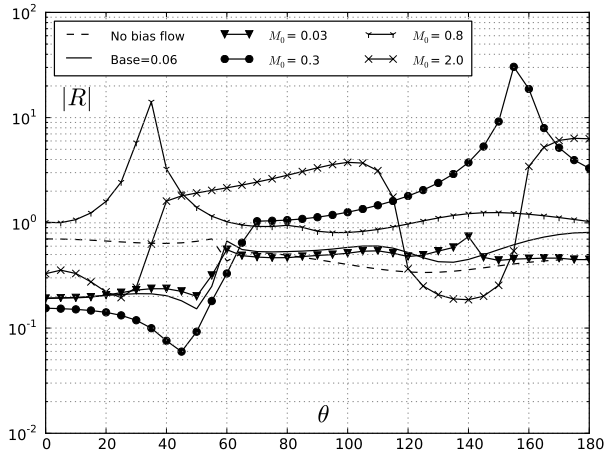

(a) Amplitude of reflection coefficient.

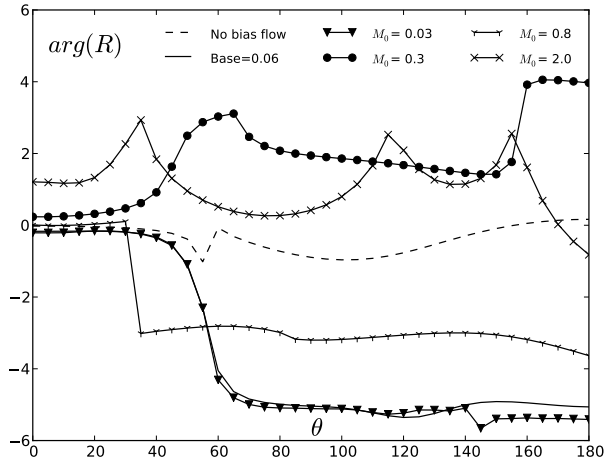

(b) Phase of reflection coefficient.

Fig. 9 : As figure 8, but using four values for cross Mach number are considered (29b) .

This is done only in one figure, figure 7. Increasing the Mach number of the cross-flow leads to a slower decay of the modulus of the acoustic pressure away from the wall (figure 7 top) as was the case increasing the core flow Mach number (figure 6 top); the phase is an almost linear function of the distance from the wall both for lower core flow (figure 6 bottom) and lower cross flow (figure 7 bottom) Mach numbers. Large cross-flow Mach numbers, well in excess of a typical bias flow, and implying a high flow rate for a fluidic jet, lead to strong sound refraction effects illustrated by non-linear amplitude and phase dependencies on the distance from the wall. The comparison of the cases with and without bias flow is made for the baseline case in the figure 7, hence for the free stream Mach number $M_\infty = 0.8$ instead of $M_\infty = 1.2$ in the figure 6. Both the amplitude (top) and the phase (bottom) of the pressure vary more slowly with the distance from the wall in the absence of the bias flow (dashed line) compared with its presence (solid line).

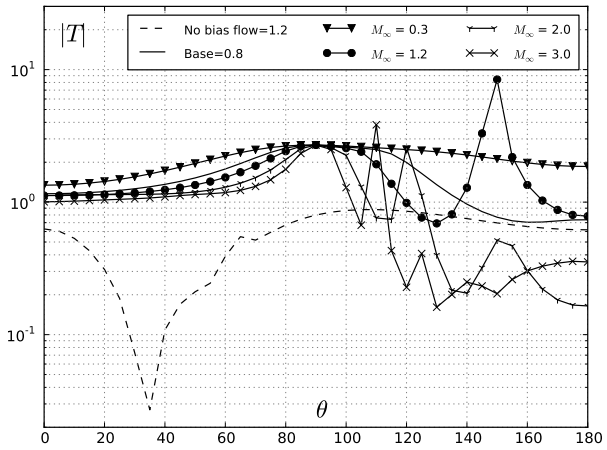

(a) Amplitude of transmission coefficient.

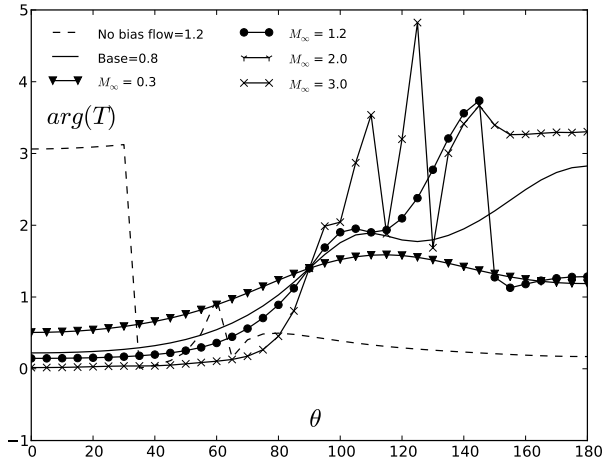

(b) Phase of transmission coefficient.

Fig. 10 : Transmission coefficient versus angle of incidence. The baseline case is used, and four values for shear Mach number are considered (29a); all with bias flow. The case without bias flow corresponds to $M_\infty = 1.2$ and is indicated by the dashed line.

Considering the reflection coefficient as a function of the angle of incidence (figures 8,9) again the amplitude and phase are plotted separately respectively at the top and bottom. The amplitude and phase are relatively smooth

(figure 8) at low free stream Mach number whereas at higher Mach numbers the interaction of the sound with the shear and bias flows leads to sharper phase changes and several amplitude peaks. The free stream Mach number $M_\infty = 1.2$ is used for the comparison of the cases without (dashed line) and with (line with circles) bias flow. The variation in the amplitude and phase of the reflection coefficient are smaller and smoother in the absence of bias flow. The increase in the Mach number of the cross flow also leads to sharper changes in the amplitude and phase of the reflection coefficient (figure 9). In the figure 9 the baseline case is used to compare the cases of no bias flow (dashed line) and bias flow (solid line); the variations of the amplitude and phase of the reflection coefficient are again smaller and smoother in the absence of bias flow. The reflection coefficient in the zone of silence is larger without bias flow.

Concerning the transmission coefficient, the amplitude and phase are again plotted separately at the top and bottom (figures 10,11) versus the angle of incidence. The transmission coefficient has severally larger amplitude and phase changes for downstream propagation and increasing free stream (figure 10) and cross flow (figure 11) Mach numbers. The comparison with the absence of the bias flow (dashed line) is made for the baseline case $M_\infty = 0.8$ (solid line) in the figure 11 and for $M_\infty = 1.2$ (line with blobs) in the figure 10. The baseline case $M_\infty = 0.8$ in the figure 11 shows that the bias flow increases the amplitude in the zone of silence, and increases the phase in the propagation zone. This is consistent with of what was seen in the figure 9 for the reflection coefficient in the zone of silence, the bias flow reduces the reflection coefficient and increases the transmission coefficient. Thus the bias flow spreads the acoustic energy over a wider range of directivities by increasing the pressure field in what would be the "zone of silence" in the absence of boundary layer. The comparison of bias flow present (line with blobs) and absent (dashed line) for a free stream Mach number $M_\infty = 1.2$ in the figure 10 shows that the modulus of transmission coefficient is increased by the bias flow in the zone of silence, and is less affected in the propagation zone, and also the phase jump at the transition between the two zones is smoothed by the bias flow.

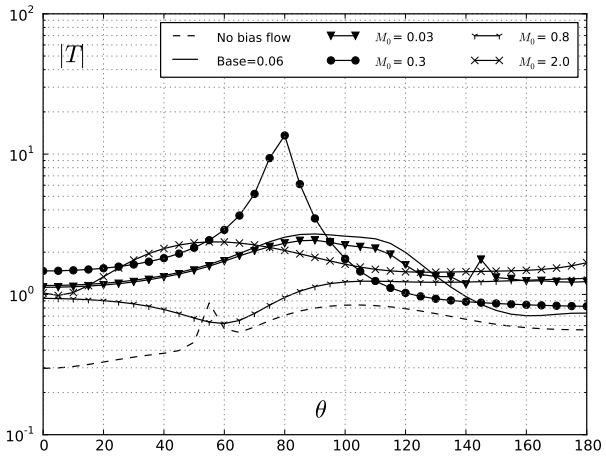

(a) Amplitude of transmission coefficient.

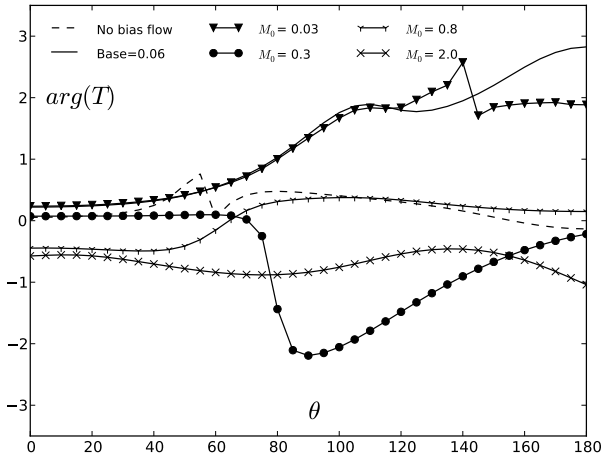

(b) Phase of transmission coefficient.

Fig. 11 : As figure 10, but using four values for cross Mach number are considered (29b) .

7 Concluding remarks

The comparison of the acoustic liner with and without bias flow shows that the mathematical consequences are: (i) the removal of the singularity at the critical layer; (ii) the increase of the order of the differential equation from two to three, implying that there is further decoupling of the acoustic and vortical modes. From the physical point-of-view the

comparison of the bias flow present and absent demonstrates changes in the modulus and phase of: (i) the acoustic pressure as a function of the distance from the wall; (ii) the reflection and transmission coefficient as a function of the angle of incidence, including different trends in the zones(s) of silence and propagation. The overall conclusion is that a bias flow with small Mach number can change significantly the acoustic pressure in the boundary layer by: (i) broadening the range of directions of propagation into the zone of silence; (ii) changing the ratio of pressure amplitudes in the free stream and at the wall. Both effects (i) and (ii) can have a beneficial effect on noise reduction, depending on the core flow, boundary layer flow and wall impedance characteristics.

8 Copyright Statement

References

[1] Campos, L.M.B.C & Serrão, P.G.T.A 1998 *On the acoustics of an exponential boundary layer.* Phil. Trans. Roy. Soc. A **356**, 2335-2379. (DOI: 10.1098/rsta.1998.0277)

[2] Campos L.M.B.C., Oliveira, J.M.G.S & Kobayashi, M.H. 1999 *On sound propagation in a linear shear flow.* J. Sound Vib. **95**, 739-770.(DOI: 10.1006/jsvi.1998.1880)

[3] Campos, L.M.B.C & Oliveira J.M.G.S. 2011 *On the acoustic modes in a duct containing a parabolic shear flow.* J. Sound Vib. **330-6**, 1166-1195.(DOI: 10.1016/j.jsv.2010.09.021)

[4] Campos, L. M. B. C., Legendre, C., & Sambuc, C. 2014. *On the acoustics of an impedance liner with shear and cross flow.* Proceedings of the Royal Society A: Mathematical, Physical and Engineering Science, 470(2163), 20130732.

[5] Forsyth, A. R. 1926 *A treatise on differential equations.* Macmillan and co., limited.

[6] Haurwitz, B. 1931 *Zur theorie der wellenbewegungen in luft und wasser.* Veroff. Geophys. Inst. Leipz. **6**, 324-364. (DOI: 10.Tam, C. K. (1998). Jet noise: since 1952. Theoretical and Computational Fluid Dynamics, 10(1-4), 393-405.1002/zamm.19320120213)

[7] Jones, D.S. 1977 *The scattering of sound by a simple shear layer.* Phil. Trans. R. Soc. Lond. A **284**, 287-328. (DOI: 10.1098/rsta.1977.0011)

[8] Küchemann, D. 1938 *Störungsbewegungen in einer Gasströmung mit Grenzschicht.* Zeits. Ang. Math. Mech. **18**, 207-221. (DOI: 10.1002/zamm.19380180402)

[9] Legendre, C. , Lielens, G. & Coyette, J-P. *Sound propagation in a sheared flow based on fluctuating total enthalpy as generalized acoustic variable.* Proceedings of the Internoise 2012/ASME NCAD meeting. New York City, NY. USA.

[10] Lilley G.M. 1973 *On the noise from jets.* AGARD Conf. Proc. **131**, 13.1-13.12.

[11] Lilley, G.M. 1974 *On the noise from air jets.* Aeronautical Research Council ARC 20376, U.K.

[12] Pridmore-Brown, D.C. 1958 *Sound propagation in a fluid flowing through an attenuating duct.* J. of Fluid Mech. **4**, 393-406.(DOI: 10.1017/S0022112058000537)

[13] Scott, J.N. 1979 *Propagation of sound waves through a linear shear layer.* Amer. Inst. Aeron. Astron. **17**, 237-245.(DOI: 10.2514/3.61107)

[14] Whittaker, E. T., & Watson, G. N. 1927. *A Course of Modern Analysis.* Cambridge U.P.